

# New technique for *in-situ* measurement of backscattered and secondary electron yields for the calculation of signal-to-noise ratio in a SEM

K. S. SIM\* & J. D. WHITE†

\*Faculty of Engineering and Technology, Multimedia University, Jalan Ayer Keroh Lama, 75450 Melaka, Malaysia

†Department of Electrical Engineering, Yuan Ze University, 135 Yuan-Tung Rd, Chung-Li, 320 Taoyuan, Taiwan

**Key words.** Scanning electron microscope, secondary electron yield, secondary emission noise, shot noise, signal-to-noise ratio.

## Summary

The quality of an image generated by a scanning electron microscope is dependent on secondary emission, which is a strong function of surface condition. Thus, empirical formulae and available databases are unable to take into account actual metrology conditions. This paper introduces a simple and reliable measurement technique to measure secondary electron yield ( $\delta$ ) and backscattered electron yield ( $\eta$ ) that is suitable for *in-situ* measurements on a specimen immediately prior to imaging. The reliability of this technique is validated on a number of homogenous surfaces. The measured electron yields are shown to be within the range of published data and the calculated signal-to-noise ratio compares favourably with that estimated from the image.

## Introduction

While it is common knowledge that the quality of an image is adversely affected by the noise level, noise in scanning electron microscope (SEM) images is notoriously difficult to handle statistically. In quantifying the signal-to-noise ratio (SNR) of SEM images, it is necessary to take into account: (1) noise in the primary beam; (2) noise due to secondary electrons; and (3) noise in the final detection system (scintillator and photomultiplier). Both Reimer (1998) and Joy (1995) have reported that the SNR is crucially dependent on the values of secondary electron yield ( $\delta$ ) and backscattered-electron yield ( $\eta$ ). Efforts to quantify and predict  $\delta$  and  $\eta$  have proceeded on a number of different fronts. Empirical formulas, such as the 'Universal Yield Curve' of Seiler (1983), have been proposed. Monte Carlo simulations of secondary electron (SE) and backscattered

electron (BSE) emission have been performed (Kotera, 1989; Ly *et al.*, 1995). Experimental databases on electron–solid interactions have been compiled (Joy, 1995). These databases comprise measurements of  $\delta$  and  $\eta$ , electron stopping powers, and X-ray ionization cross-sections as functions of energy. Although these provide important benchmarks, actual values of  $\delta$  and  $\eta$  for a given image will be different from those in the database due to sample-to-sample variations in surface condition. Measured SE yield,  $\delta$ , in particular, is very sensitive to surface conditions. Thus, in order to determine the SNR for a given image, it is necessary to measure  $\delta$  and  $\eta$  for the sample being studied, under the same conditions used to acquire the image.

Unfortunately techniques used to measure  $\delta$  and  $\eta$ , while providing accurate values, are too complicated for use on a day-to-day basis (Evenhart & Thornley, 1960; Goldstein *et al.*, 1992). Thus, SNR is often estimated based on contrast modulations within the image itself – measuring based on some kind of average signal and variation. The weakness of this approach is that the inherent contrast in the specimen will greatly affect the measurement of image SNR.

In this paper, we demonstrate a new method that is both simple and robust to measure  $\delta$  and  $\eta$  *in-situ* and is suitable for usage on a day-to-day basis. The performance of the proposed technique is tested with gold (Au), silicon (Si), aluminium (Al), copper (Cu), silver (K) and indium (In), as these materials possess different electron emission properties. Measured values of  $\delta$  and  $\eta$  are compared with those in standard databases. The SNR calculated based on the measured electron yields are then compared with the value of SNR as estimated from contrast modulations within the image.

## Theory and measurement technique

The combined specimen holder and Faraday cup used for measurement purposes is shown in Fig. 1 and illustrated schematically

Correspondence: Kok Swee Sim. Tel.: +606 252 3044; fax: +606 231 6552; e-mail: kssim@mmu.edu.my or sksbg2003@yahoo.com

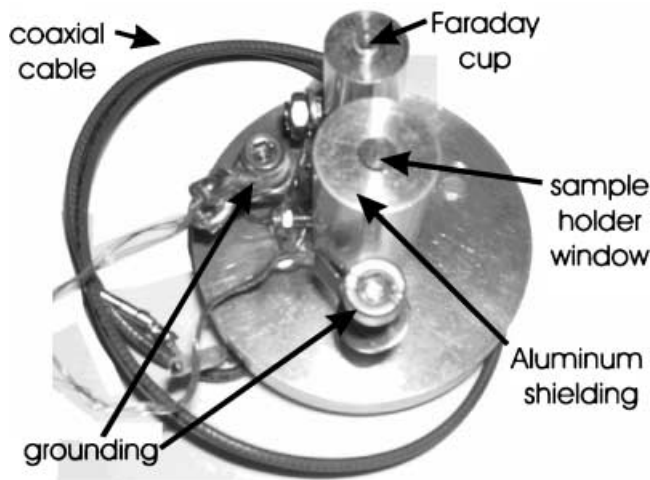


Fig. 1. Picture of the head used for image acquisition and measurement of secondary emission. The power supply and electrometer (not shown) are placed outside the SEM.

in Fig. 2. In contrast to earlier techniques which utilized an outer collector electrode or spherical grid (Reimer, 1979), the exposed area of the sample holder is minimized (Reimer, 1998). Limiting the exposed area prevents SE3 (generated by BSEs at the pole-piece and the chamber wall) from returning to the specimen. The Teflon holder isolates the specimen stub from the motorized stage of the Phillips field emission SEM (Model XL30). A simple manual switch (located outside the SEM) allows the holder to be biased at either  $\pm 45$  V using five 9 V batteries which have been carefully insulated and placed in a metal box. (Alternately a DC power supply can be used to provide  $\pm 50$  V). The specimen holder is designed with a diameter of 2.5 mm. In order to reduce electrical interference, coax cables are used as wire connections. A Keithley programmable electrometer Model 6512 is used to measure current flowing through the sample ( $I_{SC}$ ), the primary electron current ( $I_{PE}$ ) and voltage.

The primary electron (PE) current ( $I_{PE}$ ) is measured by first positioning the Faraday cup (mounted on the Teflon sample holder) in the beam path. The Faraday cup is then moved out and the specimen is placed in the beam path. With the additional measurement of the specimen current ( $I_{SC}$ ) with the specimen holder biased at positive and negative voltages,  $\delta$  and  $\eta$  can be obtained as follows:

$$I_{PE} = I_{SC} + I_{BSE} + I_{SE}$$

where  $I_{SE}$  is the SE current from all sources and  $I_{BSE}$  is the BSE current (Goldstein *et al.*, 1992). At zero biasing, SEs and BSEs are emitted from the surface. As seen in Fig. 3 (top), negatively biasing the holder ( $-45$  V) ensures that all the SEs and BSEs are repelled from the specimen. The measured specimen current ( $I_{SC,-V}$ ) is thus:

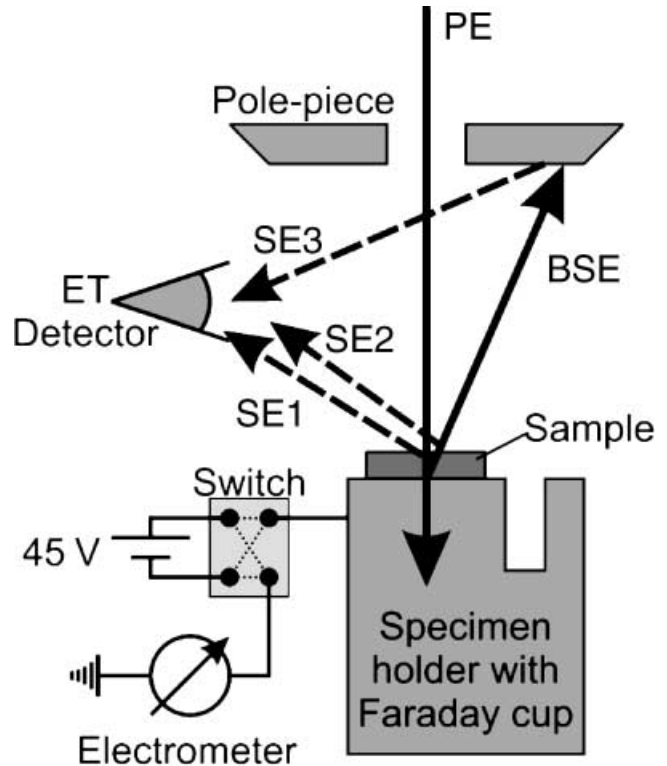


Fig. 2. Schematic diagram of set-up for the proposed SE and BSE yield measurement technique. The signal on the Everhart–Thornley (ET) detector is composed of BSE, SE1 (SE released by PE), SE2 (SE released by BSE on the object surface), and SE3 (SE released by BSE at the pole-pieces). Paths of high energy electrons are shown with solid lines, whereas paths of low energy secondary electrons are shown with dotted lines. A manual switch allows the bias on the specimen holder and Faraday cup to be reversed easily.

$$I_{SC,-V} = I_{PE} - I_{BSE} - I_{(SE1+SE2)} \quad (1)$$

where  $I_{(SE1+SE2)}$  is the current that produced from SE1 and SE2 (cf. Fig. 2). When the bias is reversed (i.e.  $+45$  V), as illustrated in Fig. 3 (bottom), low-energy SEs are attracted back to the specimen surface while BSEs continue to reach the Everhart–Thornley (ET) detector. The measured specimen current is thus given by:

$$I_{SC,+V} = I_{PE} - I_{BSE} + I_{SE3} \quad (2)$$

where  $I_{SE3}$  is the current that produced by SE3s from BSEs that hit the pole-piece.

Subtracting Eq. (1) from Eq. (2):

$$I_{(SE1+SE2)} + I_{SE3} = I_{SC,+V} - I_{SC,-V}$$

Because the present experimental set-up has been designed so that  $I_{SE3} \ll I_{(SE1+SE2)}$  (the validity of this assumption will be addressed in the Discussion section), the above equation can be approximated as:

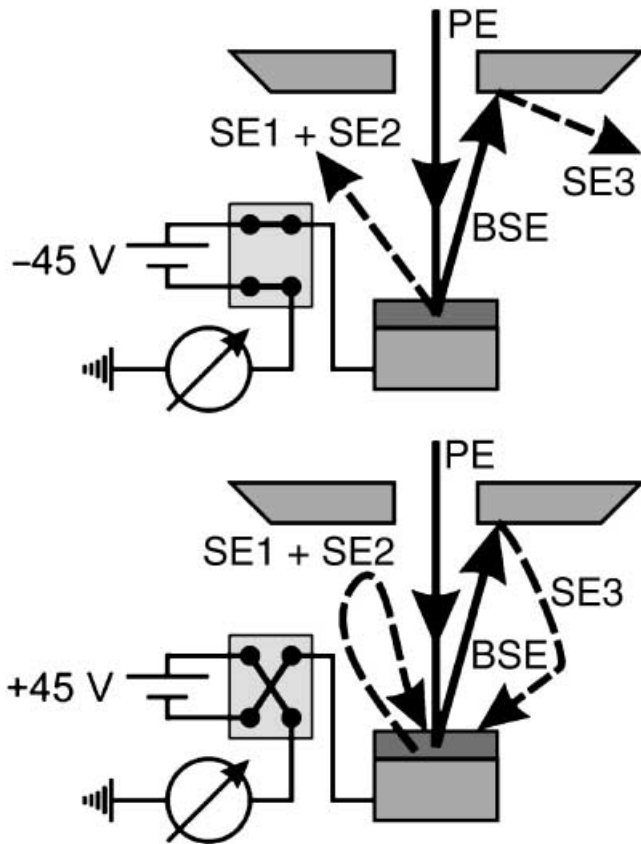


Fig. 3. Electron trajectories when a negative (top) or positive (bottom) DC bias voltage is applied to the specimen holder illustrated in Fig. 2. In the first case, SE electrons do not contribute to the current measured by the electrometer, whereas in the second case SE electrons are attracted back to the specimen and thus contribute to the measured current.

$$I_{SE} = I_{(SE1+SE2)} = I_{SC,+V} - I_{SC,-V}$$

Similarly, adding Eqs (1) and (2) and employing the same approximation, one can obtain a relationship for the BSE current:

$$I_{BSE} = I_{PE} - \frac{1}{2}(I_{SC,+V} + I_{SC,-V} + I_{(SE1+SE2)}) = I_{PE} - I_{SC,+V}$$

Thus we can write SE and BSE yield in terms of these experimental measurables as:

$$\delta = \frac{I_{SE}}{I_{PE}} = \frac{I_{SC,+V} - I_{SC,-V}}{I_{PE}} \quad \text{and} \quad \eta = \frac{I_{BSE}}{I_{PE}} = \frac{I_{PE} - I_{SC,+V}}{I_{PE}}$$

## Results

In order to validate this simple measurement technique, the SE yield ( $\delta$ ) and BSE yield ( $\eta$ ) were measured for a number of common materials and the results compared with values obtained using more sophisticated techniques. In each case

the sample surface was homogeneous. For example, in the case of gold, a homogenous sample surface was obtained by evaporating 99.9% pure gold onto a silicon wafer to give a final thickness of  $\sim 4 \mu\text{m}$ . The size of the sample was  $\sim 4 \text{mm}^2$ . Tables 1 and 2 present the measured values of BSE and SE yield, respectively, for Au, Si, Al, Cu, K and In taken at 10, 20 and 30 keV. Results are presented in comparison with published databases, with the final column providing a measurement of the difference between the values measured in this work and those by Reimer & Tolkamp (1980). For the majority of measurements, the values obtained for BSE yield differ by  $< 10\%$  from those published by Reimer & Tolkamp (1980) and are within the range of published values. In contrast for  $\delta$ , there is considerable variation ( $\sim 30\%$ ) between not only our data and that published by Reimer & Tolkamp (1980), but also within the published data itself. This variation is due to the high sensitivity of  $\delta$  on surface conditions and illustrates the necessity of measuring  $\delta$  *in-situ* rather than relying on published values.

Although the electrons are released by PEs with a range of energies, the majority of electrons have either very low or very high energy (i.e. double peaked distribution). Quite arbitrarily, those electrons with energies  $E < 50 \text{eV}$  are denoted SEs while those with  $E > 50 \text{eV}$  (i.e. elastically scattered or Auger) are denoted as BSEs (Seiler, 1983). In the data presented here, the voltage was switched between  $\pm 45 \text{V}$  in order to simplify the measurement set-up. In order to address the question of the error introduced into the comparison with published data by using  $\pm 45 \text{V}$  rather than  $\pm 50 \text{V}$ , the measurements on gold and silver were repeated making use of a switchable power supply. The difference in calculated SE and BSE yields obtained from performing measurements at  $45 \text{V}$  rather than  $50 \text{V}$  was found to be  $< 2.5\%$  in all cases.

In the previous section the approximation  $I_{SE3} \ll I_{(SE1+SE2)}$  was employed. In a rather simple experiment, the validity of this assumption is investigated. In order to block SE3, a  $2 \times 2$  inch aluminium (Al) plate was covered with carbon paint to a thickness of  $\sim 15 \mu\text{m}$ . As the Kanaya–Okayama range in carbon is  $5.3 \mu\text{m}$  at 20 keV and  $10.4 \mu\text{m}$  at 30 keV (Table 3.2 of Goldstein *et al.*, 1992), this thickness should be sufficient to absorb SE3. (The Bethe range is  $7.5 \mu\text{m}$  and  $13 \mu\text{m}$  for 20 keV and 30 keV, respectively; Goldstein *et al.*, 1992). The specimen current was measured with and without this Al plate covering the pole-piece of the SEM. The experimental results for the gold and silicon samples are summarized in Table 3. For the bright gold sample, SE3 contributes  $< 3\%$  to the total SE current, whereas for the dark silicon sample the contribution is only  $\sim 1\%$ . We conclude that for all types of samples SE3 are not significant and that the approximations employed in deriving SE and BSE yield are valid in our experimental set-up that minimizes the exposure to SE3.

Another possible source of error is current leakage. In our work this is minimized by shielding all cables. In the case of SE yield, the form of the equation ensures that a consistent underestimation of current, will, to first order, cancel out.

Material	Voltage (keV)	This study	Reimer (1980)	Other references	$\Delta$ (%)
Si	10	0.185	0.2	0.215 (Bishop, 1963)	-8
Si	20	0.18	0.194	0.104 (Bishop, 1963)	-7
Si	30	0.176	0.19	0.075 (Bishop, 1963)	-7
Al	10	0.17	0.15	NA	+13
Al	20	0.14	0.148	NA	-5
Al	30	0.12	0.144	NA	-17
Cu	10	0.29	0.311	0.339 (Bishop, 1963)	-7
Cu	20	0.28	0.311	0.339 (Bishop, 1963)	-10
Cu	30	0.28	0.311	0.319 (Bishop, 1963)	-10
K	10	0.35	0.411	0.42 (Bishop, 1963)	-15
K	20	0.35	0.415	0.419 (Bishop, 1963)	-16
K	30	0.34	0.415	0.42 (Bishop, 1963)	-18
In	10	0.36	0.419	NA	-14
In	20	0.35	0.419	NA	-16
In	30	0.34	0.419	NA	-19
Au	10	0.50	0.471	0.483 (Heinrich, 1966)	+6
Au	20	0.51	0.482	0.506 (Heinrich, 1966)	+6
Au	30	0.526	0.482	0.512 (Heinrich, 1966)	+9

**Table 1.** *In-situ* measurement of backscattered electron yield ( $\eta$ ) for various elements as a function of energy compared with published data. The sample holder was biased at  $\pm 45$  V for these measurements. The ET detector cage was biased at  $-150$  V to ensure that the ET detector would not compete for secondary electrons with voltage biasing at the specimen holder. The final column ( $\Delta$ ) is the percent difference between the measured results here and those published by Reimer & Tolkamp (1980). NA = not applicable.

Material	Voltage (keV)	This study	Reimer (1980)	Other references	$\Delta$ (%)
Si	10	0.16	0.343	0.215 (Kanter, 1961)	-53
Si	20	0.14	0.216	0.104 (Kanter, 1961)	-35
Si	30	0.09	0.138	0.075 (Kanter, 1961)	-35
Al	10	0.22	NA	0.264 (Moncrieff & Barker, 1978)	-17
Al	20	0.13	0.159	0.149 (Moncrieff & Barker, 1978)	-18
Al	30	0.11	0.096	0.137 (Moncrieff & Barker, 1978)	+15
Cu	10	0.28	NA	0.31 (Moncrieff & Barker, 1978)	-10
Cu	20	0.14	0.216	0.174 (Moncrieff & Barker, 1978)	-35
Cu	30	0.12	NA	0.161 (Moncrieff & Barker, 1978)	-25
K	10	0.25	0.358	0.285 (Moncrieff & Barker, 1978)	-30
K	20	0.23	0.264	0.236 (Moncrieff & Barker, 1978)	-13
K	30	0.19	0.157	0.214 (Moncrieff & Barker, 1978)	+21
In	10	0.33	0.3750	NA	-12
In	20	0.27	0.2850	NA	-5
In	30	0.15	0.1740	NA	-14
Au	10	0.36	0.498	0.472 (Moncrieff & Barker, 1978)	-28
Au	20	0.26	0.362	0.283 (Moncrieff & Barker, 1978)	-28
Au	30	0.18	0.253	NA	-29

**Table 2.** *In-situ* measurement of secondary electron yield ( $d$ ) for various elements as a function of energy compared with published data. The sample holder was biased at  $\pm 45$  V for these measurements. The ET detector cage was biased at  $-150$  V to ensure that the ET detector would not compete for secondary electrons with voltage biasing at the specimen holder. The final column ( $\Delta$ ) is the percent difference between the measured results here and those published by Reimer & Tolkamp (1980) where available. Where not available, we have compared the results with other published references. NA = not applicable.

### Electron yield and SNR

SNR is the sum of the contributions of PE, SE and BSE sources of noise. For an SEM equipped with a thermionic electron gun, shot noise is the dominant noise source in the PE beam (Dubbeldam & Thong, 1993) and follows Poisson statistics (Reimer, 1998). Concerning BSE, whereas the conversion from PE to BSE follows a binomial distribution, the combination of the Poisson statistics of PE with the binomial conversion gives BSE emission a Poisson distribution. In the following discussion we follow the derivation used by Reimer (1998) to determine SNR based on knowledge of  $I_{PE}$ ,  $\delta$ ,  $\eta$  and the acquisition time per pixel of the digital image ( $\tau$ ). The mean number

of PEs per pixel is  $\bar{N}_{PE} = I_{PE}\tau/e$ , where  $e$  is the charge on a single electron. The SNR of primary electrons is thus:

$$SNR_{PE} = \bar{N}_{PE}/[\text{var}(N_{PE})]^{1/2} = \bar{N}_{PE}^{1/2}.$$

Similarly for BSEs the cascade of the Poisson distribution of the PE and the binomial distribution of conversion factor  $\eta$  yields:

$$SNR_{BSE} = \bar{N}_{PE}\eta/[\text{var}(\bar{N}_{PE}\eta)]^{1/2} = (\bar{N}_{PE}\eta)^{1/2}.$$

Unfortunately, noise contributed by SEs cannot be so simply handled. The distribution is neither Poisson nor binomial

**Table 3.** Measurement of specimen current ( $I_{sc}$ ) measured with the electrometer for silicon and gold specimens with and without suppression of the SE3 contribution. The final column gives the percent contribution of SE3 to the total specimen current

Target specimen	Specimen current ( $I_{sc}$ ) (nA)		SE3 contribution (%)
	No plate	Cover in	
Si	-0.278	-0.275	1
Au	-0.177	-0.172	3

because one PE can release zero, one or more SEs with decreasing probability (Goldstein *et al.*, 1992). Thus:

$$\text{SNR}_{SE} = \bar{N}_{PE} \delta / [\text{var}(\bar{N}_{PE} \delta)]^{1/2} = [\bar{N}_{PE} / (1 + b)]^{1/2},$$

where  $b \equiv \text{var}(\delta) / \delta^2$ . In the limiting case of Poisson statistics,  $\text{var}(\delta) = \delta$  and thus  $b = 1/\delta$ . The deviation from Poisson statistics results in an increase in  $b$  by a factor of 1.2 (Al) to 1.5 (Au), depending on the material and electron energy. Thus, using the known values of  $I_{PE}$  and  $\tau$ , the measured value of  $\eta$  or  $\delta$ , the SNR for images based on BSEs or SEs, respectively, can be determined. In the second case, one also needs to include the material-dependent noise enhancement. Finally the value of SNR measured by the ET detector is less than that derived from the incident electron dose and the relevant electron yield factor. This is primarily because the finite quantum efficiency (DQE) of the ET detector (Faraday cage  $\rightarrow$  scintillator  $\rightarrow$  photomultiplier tube) will result in a reduction in SNR according to the relationship (Jones, 1959):

$$\text{SNR}_{ET} = \sqrt{\text{DQE}} \times \text{SNR}_{\text{yield}}$$

The DQE or collection efficiency only needs to be measured once for a given microscope/detector. The method involved has been described adequately in the literature and is beyond the scope of this paper (Joy *et al.*, 1996). We estimate the DQE of our instrument to be 0.23. This is within the range of published values of between 0.15 and 0.25 (Jones, 1959; Joy *et al.*, 1996) for this instrument. The calculated SNR for images generated by SE emission for the silicon and gold specimens is summarized in Tables 4 and 5, respectively, as a function of electron energy. The values obtained for SNR are remarkably constant over the voltage range studied, despite a 50% drop in SE yield at higher incident energies.

In experimental work, the SNR of an image is often estimated from the image itself according to the relationship:  $\text{SNR} = (I_{\text{mean}} - I_{DC}) / \sigma$ , where  $I_{\text{mean}}$  is the mean intensity of the image averaged over all the pixels,  $\sigma$  is the standard deviation of the intensity recorded at each pixel, and  $I_{DC}$  is the mean intensity of the image averaged over all the pixels at zero beam current. Experimentally,  $I_{DC}$  is obtained during system calibration prior to carrying out digital imaging. Such calibration is necessary

**Table 4.** Comparison of SNR derived from secondary electron yield compared with that estimated from the image for homogeneous silicon (Si) specimen. The DQE of our instrument was estimated to be 0.23. The deviation from Poisson statistics resulted in an enhancement in  $b$  of a factor of 1.3. The acquisition time per pixel ( $\tau$ ) was 7.81  $\mu\text{s}$

Voltage (keV)	SNR based on electron yield				SNR from image			
	$\delta$	$I_{PE}$ (pA)	$\text{SNR}_{SE}$	$\text{SNR}_{ET}$	$I_{DC}$	$I_{\text{mean}}$	$\sigma$	$\text{SNR}_{ET}$
10	0.16	291	40	19	12.1	68	2.35	24
20	0.14	371	42	20	12.3	45	1.72	19
30	0.09	495	40	19	11.8	41	1.35	22

**Table 5.** Comparison of SNR derived from secondary electron yield compared with that estimated from the image for homogeneous gold specimen. The DQE of our instrument was estimated to be 0.23. The deviation from Poisson statistics resulted in an enhancement in  $b$  of a factor of 1.3. The acquisition time per pixel ( $\tau$ ) was 7.81  $\mu\text{s}$

Voltage (keV)	SNR based on electron yield				SNR from image			
	$\delta$	$I_{PE}$ [pA]	$\text{SNR}_{SE}$	$\text{SNR}_{ET}$	$I_{DC}$	$I_{\text{mean}}$	$\sigma$	$\text{SNR}_{ET}$
10	0.36	291	52	25	11.9	121.3	3.35	33
20	0.26	371	52	25	12.1	108.8	3.15	31
30	0.18	495	51	24	12.3	98.2	2.98	29

to ensure that measurement results do not saturate at either the top or the bottom of the video dynamic range. A convenient procedure to achieve this (and simultaneously obtain  $I_{DC}$ ) is to control the incident beam current with the aperture of the SEM. The SEM aperture is first adjusted so that the signal is as close to zero as possible, and an image is captured. Next, the aperture is sequentially switched from the largest to the smallest available diameter over a period of few seconds during the scan and the incident beam current at each setting is recorded. From the image, the mean intensity corresponding to each beam current is calculated. In Fig. 4, plots of  $I_{\text{mean}}$  as a function of beam current are shown for both the Au and Si samples. The slope clearly varies between samples, with the mean intensity for Au being more dependent on beam current. Both plots are linear, with no saturation evident at this value of PE current. The values of  $I_{DC}$ , obtained from the  $y$ -axis intercepts, are 12.3 and 12.1 for Au and Si, respectively.

Tables 4 and 5 compare the SNR of images based on SEs calculated using the SE yield with that estimated from the image itself for silicon and gold at three different voltages. Comparing the calculated and estimated SNR, one notes that there is must greater variation with electron energy in the SNR estimated from the images than that calculated based on electron yield. Secondly, the difference between SNR (averaged over electron energy) is  $\sim 10\%$  for the silicon specimen and  $\sim 20\%$  for the gold specimen. A number of factors may be responsible for

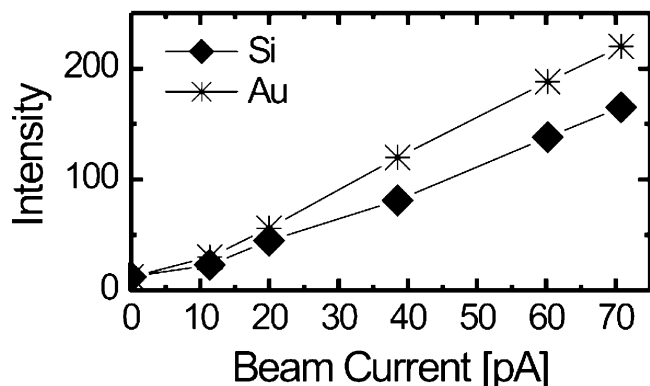


Fig. 4. Mean image intensity as a function of beam current for Au and Si at  $I_{PE} = 379$  pA taken at 20 keV. Experimental data are shown as stars (Au) and diamonds (Si). The  $y$ -axis intercepts are 12.3 and 12.1 for Au and Si, respectively.

these deviations. First, it is possible that we have overestimated the enhancement of  $b$  due to non-Poisson statistics. If Poisson statistics are assumed to hold, then the two calculation methods agree to within 5%. Secondly, although SE3s do not affect the SE yield measurement, they may affect the image SNR. Thirdly, for an ideal SE detector, 100% of the emitted SEs arrive at the detector, whereas no BSEs are detected. In reality, a small amount of BSEs will be detected and these may influence the SNR either positively or negatively.

The results summarized in Tables 4 and 5 may lead to the conclusion that the SNR estimated from the image is always equivalent to that calculated making use of electron yields. Although this is generally true for a perfectly homogeneous specimen surface, any real contrast in the image will lower the apparent SNR. For example, in a high contrast image,  $\sigma$  will be large, resulting in an artificially low value for SNR. Calculating SNR from electron yield eliminates this convolution.

## Conclusions

In this paper it is shown that knowledge of the PE current and specimen current with the sample holder biased at  $\pm 45$  V was sufficient to determine both SE ( $\delta$ ) and BSE ( $\eta$ ) yield. Based on this observation, a simple and robust set-up for the *in-situ* determination of  $\delta$  and  $\eta$  was described and implemented. Measured values were shown to be within the existing range

of the published databases. The SNR calculated based on SE yield was shown to be comparable to the SNR estimated from the image for a homogeneous specimen. This technique will be useful in evaluating SNR for situations in which the sample surface condition varies greatly from that used in the calculation of the published databases or where the specimen itself possesses high inherent contrast. The simplicity of the technique makes it suitable for day-to-day use.

## References

- Bishop, H.E. (1963) *Electron scattering and X-ray production*. PhD Thesis, University of Cambridge, Cambridge.
- Dubbeldam, L. (1993) *Electron Beam Interaction with Specimen* (ed. by J. T. L. Thong), pp. 218–223. Plenum Press, New York.
- Evenhart, T.E. & Thornley, R.F.M. (1960) Wide band detector for microampere low-energy electron currents. *J. Sci. Instrum.* **37**, 246.
- Goldstein, J.L., Newbury, D.E., Echlin, P., Joy, D.C., Roming, A.D. Jr, Lyman, C.E., Fiori, C. & Lifshin, E. (1992) *Scanning Electron Microscopy and X-Ray Microanalysis: A Text for Biologists, Material Scientists and Geologists*, 2nd edn. Plenum Press, New York.
- Heinrich, K.E.J. (1966) X-ray optics and microanalysis. *Proceedings of the 4th Conference on X-ray Optics and Microanalysis* (ed. by R. Castaing, P. Descamps & J. Philibert), p. 159. Hermann, Paris.
- Jones, R.C. (1959) The statistics of electron detection. *Adv. Electronics Electron Optics*, **11**, 88–108.
- Joy, D.C. (1995) A database on electron–solid interactions. *Scanning*, **17**, 270–275.
- Joy, D.C., Joy, C.S. & Bunn, R.D. (1996) Measuring the performance of scanning electron microscope detectors. *Scanning*, **18**, 533–538.
- Kanter, H. (1961) Contribution of backscattered electrons to secondary electron formation. *Phys. Rev.* **121**, 681–684.
- Kotera, M. (1989) A Monte Carlo simulation of primary and secondary electron trajectories in a specimen. *J. Appl. Phys.* **65**, 3991–3998.
- Ly, T.D., Howitt, D.G., Farrens, M.K. & Harker, A.B. (1995) Monte Carlo calculation for specimens with microstructures. *Scanning*, **17**, 220–226.
- Moncrieff, D.A. & Barker, P.R. (1978) Secondary electron emission in the scanning electron microscope. *Scanning*, **1**, 195–197.
- Reimer, L. (1979) Electron–specimen interactions. *Scanning Electron Microsc. II*, 111–124.
- Reimer, L. (1998) *Scanning Electron Microscopy: Physics of Image Formation and Microanalysis*, 2nd edn. Springer Series in Optical Sciences. Springer, Berlin.
- Reimer, L. & Tolkamp, C. (1980) Measuring the backscattering coefficient and secondary electron yield inside a SEM. *Scanning*, **3**, 35.
- Seiler, H. (1983) Secondary electron emission in the scanning electron microscope. *J. Appl. Phys.* **54**, R1–R18.